Impact of temperature dependence on the possible contribution of organics to new particle formation in the atmosphere

Fangqun Yu[1], Gan Luo[1], Alexey B. Nadykto[1, 2], and Jason Herb[1]

[1]Atmospheric Sciences Research Center, State University of New York, 251 Fuller Road, Albany, New York 12203, USA

[2]Department of Applied Mathematics, Moscow State University of Technology "Stankin", Vadkovsky 1, Moscow, Russia

Abstract. Secondary particles formed via new particle formation (NPF) dominate cloud condensation nuclei (CCN) abundance in most parts of the troposphere and are important for aerosol indirect radiative forcing (IRF). Laboratory measurements have shown that certain organic compounds can significantly enhance binary nucleation of sulfuric acid and H_2O. According to our recent study comparing particle size distributions measured in nine forest areas in North America with those predicted by a global size-resolved aerosol model, current H_2SO_4-Organics nucleation parameterizations appear to significantly over-predict NPF and particle number concentrations in summer. The lack of the temperature dependence in the current H_2SO_4-Organics nucleation parameterization has been suggested to be a possible reason for the observed over-prediction. In this work, H_2SO_4-Organics clustering thermodynamics from quantum-chemical studies has been employed to develop a scheme to incorporate temperature dependence into H_2SO_4-Organics nucleation parameterization. We show that temperature has a strong impact on H_2SO_4-Organics nucleation rates, and may reduce nucleation rate by ~ one order of magnitude per 10 K of the temperature increase. The particle number concentrations in summer over North America based on the revised scheme is a factor of more than two lower, in much better agreement with the observations. With the temperature-dependent H_2SO_4-Organics nucleation parameterization, the summer month CCN concentrations in the lower troposphere in the northern hemisphere are about 10-30% lower compared to the temperature independent one. This study highlights the importance of the temperature effect and its impacts on NPF in global modeling of aerosol number abundance.

1. Introduction

Atmospheric particles, through acting as cloud condensation nuclei (CCN), modify cloud properties and precipitation and thus, indirectly, affect the hydrological cycle and climate. Aerosol indirect radiative forcing (IRF) remains a major uncertainty in assessing climate change (IPCC, 2013). Secondary particles formed via nucleation dominate particle number concentrations in many parts of troposphere (Spracklen et al., 2008; Pierce and Adams, 2009; Yu and Luo, 2009), and global simulations indicate that nucleation schemes/parameterizations have a strong effect on the aerosol IRF estimations (Wang and Penner, 2009; Kazil et al., 2010; Yu et al., 2012). Different nucleation schemes, with nucleation rates depending on different variables, predict significantly different spatial patterns and seasonal variations of nucleation rates and CCN concentrations (Yu et al., 2010, 2015). Therefore, it is important to understand mechanisms of new particle formation (NPF) and the key parameters controlling the contribution of the NPF to CCN formation under wide range of varying atmospheric conditions and to validate their representation in regional and global climate models.

A number of laboratory chamber studies indicate that certain organic species can significantly enhance NPF (e.g., Zhang et al., 2004; Riccobono et al., 2014). This finding may have important implications for the interactions of anthropogenic and biogenic emissions and the associated climate forcing. To this regard, it is necessary to assess the ability of organics-enhanced nucleation to explain nucleation phenomena observed in the atmosphere and to determine the contribution of organics to atmospheric NPF and climate implications. In several laboratory studies, empirical parameterization of formation rate as a function of the concentrations of sulfuric acid and low-volatility highly oxidized organics has been derived (Metzger et al., 2010; Riccobono et al., 2014). One of the most important limitations of these

empirical parameterizations is that they were derived from the chamber measurements carried out under limited range of well-controlled conditions and, thus, reliably extrapolating these data to a wide range of atmospheric conditions remains a major issue. It should also be noted that empirical activation and kinetic nucleation formulas ($J = k_1[H_2SO_4]$ or $J = k_2[H_2SO_4]^2$) derived from limited field measurements (e.g., Riipinen et al., 2007; Kuang et al., 2008) also do not account for the impact of temperature variations on computed nucleation rates. Although these simple empirical temperature independent nucleation parameterizations have been widely used in global aerosol modeling and aerosol IRF studies (e.g., Spracklen et al., 2008; Wang and Penner, 2009; Kazil et al., 2010; Scott et al., 2014; Westervelt et al., 2014; Lupascu et al., 2015), possible impacts of temperature variations were not considered in these studies.

In a recent study comparing particle size distributions measured in nine forest areas in North America with those predicted by a global size-resolved (sectional) aerosol model, Yu et al. (2015) showed that H_2SO_4-Organics nucleation parameterization of Riccobono et al. (2014) significantly over-predict NPF and particle number concentrations in summer (Yu et al., 2005). The lack of temperature dependence in the H_2SO_4-Organics nucleation parameterization has been suggested as a possible reason for the observed over-prediction. The main objectives of the present study are (1) to develop a scheme to incorporate temperature dependence into H_2SO_4-Organics nucleation parameterization, (2) to assess the ability of the modified parameterization in explaining the seasonal variations of NPF in NA, and (3) to study the global implications.

2. Methods

2.1. Organics-mediated nucleation parameterization with temperature dependence (Nucl-OrgT)

Based on the CLOUD chamber study of nucleation process involving sulfuric acid and organic compounds of relatively low volatility from the oxidation of pinanediol, Riccobono et al. (2014) derived the following organics-mediated nucleation parameterization (Nucl-Org),

$$J_{Nucl\text{-}Org} = k_m \times [H_2SO_4]^2 \times [BioOxOrg] \quad (1)$$

where $J_{Nucl\text{-}Org}$ is the formation rate (# $cm^{-3}s^{-1}$) of particles of ~ 1.7 nm, k_m is the fitting pre-factor with a value of 3.27×10^{-21} cm^6 s^{-1} (90% confidence interval: 1.73×10^{-21} to 6.15×10^{-21} cm^6 s^{-1}), $[H_2SO_4]$ and [BioOxOrg] are the gas-phase concentrations (# cm^{-3}) of H_2SO_4 and biogenic oxidized organic (BioOxOrg) vapors, respectively. In the chamber study reported in Riccobono et al. (2014), BioOxOrg molecules are organic compounds of relatively low volatility from the oxidation of pinanediol (a first-generation oxidation product of α-pinene) and represent later-generation oxidation products of biogenic monoterpenes.

The Nucl-Org parameterization given in Eq. 1, derived from laboratory chamber studies at T=278 K and RH=39% (Riccobono et al., 2014), does not consider the possible effect of temperature on nucleation rate. According to the nucleation theory, nucleation rates are temperature-dependent unless nucleation is barrierless and limited by collision rates only. However, the value of the pre-factor k_m of 3.27×10^{-21} cm^6 s^{-1} is well below the three-body collision rate corresponding to the formation of a cluster containing two H_2SO_4 and one BioOxOrg molecules. This indicates that nucleation in the CLOUD chamber under conditions reported in Riccobono et al. (2014) was not barrierless, and, thus, nucleation rates should be temperature-dependent.

Based on the classical homogeneous nucleation theory, the rate of nucleation (J) can be generally written in the form

$$J = C_1 \exp(-\Delta G/kT) \quad (2)$$

where ΔG is the Gibbs free energy needed to form the critical cluster and C_1 is the pre-factor. With ΔG = ΔH - T ΔS, where ΔH and ΔS are associated enthalpy and entropy change, we get

$$J = C_1 \exp(-\Delta H/kT + \Delta S/k) = C_1 \exp(\Delta S/k) \exp(-\Delta H/kT) = C_2 \exp(-\Delta H/kT) \quad (3)$$

The temperature dependence of nucleation rate is dominated by the exponential term in Eq. (3), although C_2 may also weakly depend on temperature. Assuming that C_2 is independent of temperature and using $J_{Nucl\text{-}Org}$ given in Eq. (1) as the nucleation rate at the reference temperature T_0=278 K, we obtain

$$J_{Nucl\text{-}OrgT} = J_{Nucl\text{-}Org}\ f_T \quad (4)$$

$$f_T = \exp[\frac{\Delta H}{k}(\frac{1}{T} - \frac{1}{T_0})] \quad (5)$$

where f_T is the correction factor accounting for the temperature dependence.

One challenge here is to obtain enthalpy change (ΔH) associated with the critical cluster formation because it is quite difficult to determine the chemical identities of BioOxOrg molecules involved in atmospheric nucleation (Elm et al, 2014; Riccobono et al., 2014). As a first order approximation, we use 2-Methyl-5-[(1S,2S,3R)-1,2,3,4-tetrahydroxybutyl]-3-furoic acid, a select highly oxidized organic $C_{10}H_{14}O_7$ compound, as a proxy for BioOxOrg molecules. The stability of the cluster composed of two H_2SO_4 and one $C_{10}H_{14}O_7$ molecules has been investigated using the Density Functional theory (DFT) at PW91PW91/6-311++G(3df,3pd) level. The PW91PW91 is the most common density functional used in atmospheric studies that predicts structure, vibrational spectrums, dipolar properties and thermodynamics of atmospheric molecules and molecular clusters with high degree of confidence and its predictions, which have been systematically validated against experimental and higher level ab initio Gibbs free energies, are in a very good agreement with them for a number of atmospherically relevant molecules and

124 clusters (e.g. Herb et al., 2013, Elm et al., 2013, Nadykto et al., 2015; DePalma et al., 2015).
125 Computations have been carried out using the Gaussian 09 suite of programs (Frish et al., 2009).

126 Figure 1 presents the equilibrium geometry of the most stable isomers of heteromolecular
127 trimer composed of $(C_{10}H_{14}O_7)(H_2SO_4)_2$ and Table 1 reports the corresponding the
128 thermodynamic data associated the formation of this cluster. The computational methodology,
129 benchmarks of Gibbs free energy changes and Cartesian geometries of global minima and local
130 minima located within 1 kcal mol^{-1} of the global minima, along with interactions of $C_{10}H_{14}O_7$
131 and H_2SO_4 with some base molecules, will be detailed in a separate manuscript. Here, as a first
132 order of approximation, we use ΔH value of -38.30 kcal mol^{-1} to calculate the temperature-
133 dependent factor f_T in Eq. (5). Figure 2 shows the calculated value of f_T as a function of T. It is
134 clear from Fig. 2 that f_T decreases significantly as T increases, roughly one order of magnitude
135 per 10 K. When T < 269 K, f_T becomes larger than 10 and increases with decreasing T. f_T is set
136 to have a maximum value so that $J_{Nucl\text{-}OrgT}$ does not exceed the 3-body kinetic collision rate for
137 forming a cluster containing two H_2SO_4 molecules and one BioOxOrg molecule, which depends
138 on T as well as the mass and sizes of colliding molecules. At T=270 K, the maximum value of f_T
139 is ~ 38. Compared to the original $J_{Nucl\text{-}Org}$ parameterization of Riccobono et al. (2014) (Eq. 1)
140 derived from laboratory chamber studies at T=278 K and not taking into account the temperature
141 dependence of nucleation rates (i.e., f_T =1, dashed line in Fig. 2), the revised parameterization
142 $J_{Nucl\text{-}OrgT} = f_T J_{Nucl\text{-}Org}$ predicts quite different nucleation rate in the atmosphere, especially in the
143 summer season, when both T and VOC emissions are at peak values.

144 It should be noted that f_T shown in Fig. 2 is subject to large uncertainty because of the
145 potential difference between the molecules involved in the nucleation and the proxy molecule
146 shown in Figure 1. The thermodynamic data for the formation of $(H_2SO_4)_2$(BioOxOrg) clusters is

147 quite limited. Elm et al. (2014) investigated the molecular interactions between the α-pinene
148 oxidation product pinic acid and sulfuric acid using computational methods and reported a ΔH
149 value of -42.5 kcal/mol for the formation of $(H_2SO_4)_2$(Pinic Acid). More negative ΔH implies
150 stronger temperature dependence. The sensitivity of f_T values to ΔH can be readily calculated
151 from Eq. (4). For example, a fairly large uncertainty of 5 kcal mol^{-1} in ΔH leads to the
152 uncertainty in f_T of a factor of ~ 1.4 at T=288 K, while the extremely large 20 kcal mol^{-1}
153 variation in ΔH alters f_T at T=288 K by a factor of ~ 3.5. The sensitivity of predicted nucleation
154 rates and particle number concentrations to ΔH values is presented in Section 3. Despite possible
155 uncertainties in f_T, the temperature dependent $J_{Nucl\text{-}OrgT}$ is likely to be more realistic than $J_{Nucl\text{-}Org}$,
156 in which the temperature dependence is neglected.
157
158 2.2. GEOS-Chem model and global simulations
159 This work represents a major global modeling attempt in studying the effect of temperature
160 on organics-mediated nucleation in the atmosphere. This study is built upon the work reported in
161 Yu et al. (2015) and, thus, we use the same global model (GEOS-Chem) and configurations as
162 that described in Yu et al. (2015). GEOS-Chem is a global 3-D model of atmospheric
163 composition driven by assimilated meteorological observations from the Goddard Earth
164 Observing System (GEOS) of the NASA Global Modeling and Assimilation Office (GMAO)
165 (e.g., Bey et al., 2001). More detailed information about GEOS-Chem and updates can be found
166 at the model website (http://geos-chem.org/). The aerosol simulation is based on a size-resolved
167 (sectional) advanced particle microphysics (APM) model incorporated into GESO-Chem by Yu
168 and Luo (2009) and considers the successive oxidation aging of the oxidation products of various
169 VOCs (Yu, 2011). In GEOS-Chem v8-03-02, on which this study and previous work (Yu et al.,

2015) are based, the concentration of highly oxidized low volatile secondary organic gas from the oxidation products of α-pinenes ($LV\text{-}SOG_{\alpha\text{-pinene}}$) is explicitly simulated and used in Eqs. (1) and (4) to calculate organics-mediated nucleation rates. The horizontal resolution of GEOS-Chem employed in this study is $2^o \times 2.5^o$ and there are 47 vertical model layers (with 14 layers from surface to ~ 2 km above the surface). Other relevant model configurations (including emission inventories and various schemes) can be found in Yu et al. (2015).

The main difference between the present study and the previous one reported by Yu et al. (2015) is that the present study employs the T-dependent Nucl-Org parameterization given in Eq. (4) instead of T-independent parameterization of Riccobono et al. (2014). In addition, study of Yu et al. (2015) focuses only on the NA region, while in this work, the discussion on organics-mediated nucleation is expanded to the whole globe.

3. Results

Figure 3 shows the effect of T-dependent correction factor on simulated global distributions of monthly mean (July, 2006) nucleation rates, particle number and CCN concentrations in the boundary layer (0-1 km above the surface). The high biogenic VOC emissions in the summer coupled with strong photochemistry lead to higher concentrations of $LV\text{-}SOG_{\alpha\text{-pinene}}$ or BioOxOrg (Yu et al., 2015) and hence, according to the parameterization of Riccobono et al. (2014) (i.e., Eq. 1), significant organics-mediated nucleation (Fig. 3a) and higher particle number concentrations (Figs. 3c and 3e). However, the high temperature in the summer substantially lower nucleation rates (Fig. 3b), and reduce the global monthly mean nucleation rate in the boundary layer from 0.17 $cm^{-3}s^{-1}$ (Fig. 3a) to 0.02 $cm^{-3}s^{-1}$, with stronger effect in the northern

192 hemisphere (Fig. 3b). As a result, the global monthly mean CN10 and CCN0.4 in the boundary
193 layer decrease by 40% and 30%, respectively.

194 A ΔH value of -38.3 kcal mol^{-1} was used in calculating $J_{Nucl\text{-}OrgT}$ in Fig. 3b. The impact of ΔH
195 values (from 0 to 58.3 kcal mol^{-1}) on $J_{Nucl\text{-}OrgT}$, CN10 and CCN0.4 averaged in the boundary
196 layer over the whole globe for the same summer month is presented in Figure 4. A zero value of
197 ΔH corresponds to the case of no T-dependent correction (i.e., $J_{Nucl\text{-}Org}$, Fig. 3a). $J_{Nucl\text{-}OrgT}$, CN10
198 and CCN0.4 are more sensitive to ΔH when ΔH is small (<~ 30 kcal mol^{-1}), with $J_{Nucl\text{-}OrgT}$
199 decreasing by a factor of 5, CN10 by 33% and CCN0.4 by 28% as ΔH increases from 0 to 28.3
200 kcal mol^{-1}. Further increase of ΔH from 28.3 to 58.3 kcal mol^{-1} reduces $J_{Nucl\text{-}OrgT}$, CN10 and
201 CCN0.4 by 100%, 25%, and 10%, respectively. It can be seen from Figure 4 that the T-
202 dependent correction, even with a smaller value of ΔH, is important. On the other hand, the
203 effect of potential uncertainty in ΔH around the values derived from quantum calculation (~ 40
204 kcal mol^{-1}, see Section 2.1) is relatively weaker.

205 As we have pointed out earlier, the previous comparisons of simulated and observed particle
206 size distributions measured in nine forest areas in North America (NA) (Yu et al., 2005) showed
207 that $J_{Nucl\text{-}Org}$ parameterization (Eq. 1) over-predicts condensation nuclei number concentrations in
208 the size range of 10 and 100 nm ($CN_{10\text{-}100}$) at these sites in summer by a factor of around two on
209 average (Yu et al., 2005). To examine the extent, at which the revised parameterization
210 considering T-dependence (Eq. 4) can improve the agreement of simulations with measurements,
211 we present the monthly mean horizontal distributions of CN10 zoomed into the NA region in Fig.
212 5 and observed and simulated $CN_{10\text{-}100}$ averaged over the nine forest sites in Fig. 6. It can be
213 clearly seen from Fig. 5 that the simulated monthly mean CN10 values in the NA boundary layer
214 based on $J_{Nucl\text{-}OrgT}$ (Eq. 4) are about a factor of two lower than those based on $J_{Nucl\text{-}Org}$ (Eq. 1),

with larger difference in the lower latitude part of the domain, where T is higher. In the case, when the effect of T on Nucl-Org is taken into account, the domain-wide average CN10 value decreases from 4600 to 2200 #/cm^3 and Figure 6 shows that the simulated $CN_{10\text{-}100}$ averaged over the nine forest sites (with locations marked on Fig. 5, see Yu et al. (2015) for details) agrees much better with that of observed. It can also be seem from Fig. 6 that $CN_{10\text{-}100}$ over the NA forest sites is more sensitive to ΔH values than the global mean CN10 shown in Fig. 4, and ΔH of ~35 kcal mol^{-1} agrees best with the observations.

To further illustrate the difference and improvement for the cases with and without T-dependent correction, we present in Fig. 7 a set of detailed comparisons of simulated and observed evolution of particle size distributions during two ten-day periods in March and July of 2006 in Duke Forest (Pillai et al., 2013), along with time series of $CN_{10\text{-}100}$ (integrated from PSDs), which give a good overall representation of particle nucleation and growth. The observed PSDs and simulated PSDs based on $J_{Nucl\text{-}Org}$ has been discussed in Yu et al. (2015) and are repeated here for comparison with $J_{Nucl\text{-}OrgT}$ scheme in order to demonstrate the impact of temperature on nucleation and particle number concentrations. Although the present work focuses on the summer month, when the largest difference between $J_{Nucl\text{-}Org}$ prediction and observation is observed, we also show in Fig. 7 simulations for a 10-day period in March as well for the comparison purpose. NPF events observed in Duke Forest are much more frequent and concentrations of nucleation mode particles are much higher in the spring than in the summer (Figs. 7a & 7b). The temperature correction (Eq. 4) has small effect in the spring (Figs. 7c, 7e, and 7g) but significantly reduces nucleation rate and particle number concentration in summer (Figs. 7d, 7e, and 7f). $J_{Nucl\text{-}Org}$ scheme (Eq. 1) predicts strong nucleation events (Fig. 7d) and significant diurnal variations in $CN_{10\text{-}100}$ (Fig. 7h) almost every day in the summer period that

obviously contradicts to observations (Fig. 7b). The high nucleation rates in the summer based on $J_{Nucl\text{-}Org}$ scheme can be easily explained by the much higher BioOxOrg concentrations as a result of high VOC emissions and stronger photochemistry. Nevertheless, the high T in the summer inhibits nucleation (Eq. 4) and the temperature correction factor substantially improves the agreement of the simulated evolution of PSDs (Figs. 7b, 7d, 7f) and $CN_{10\text{-}100}$ (Fig. 7h) with observations.

Figure 8 shows the ratios of the CCN concentration in the lower troposphere (0-3 km) based on Nucl-Org to the CCN concentration based on Nucl-OrgT. The CCN concentrations are calculated at a water supersaturation ratio of 0.2% (CCN0.2) from simulated PSDs. As a result of higher nucleation rates, CCN0.2 based on Nucl-Org are about 10-20% higher than those based on Nucl-OrgT in July over most parts of northern hemisphere (Fig. 6a), with the largest difference up to 30-70% reached over part of NA, Europe, and Asia. It is noteworthy that the present model simulation only considers the Nucl-Org parameterization. While this enables us to show more unambiguously the effect of T-dependent correction, it may overestimate the sensitivity of CCN to changes in the nucleation rate as a result of atmospheric saturation when all nucleation mechanisms (including non-organic nucleation) are present. Further simulation including all individually verified nucleation mechanisms is needed to evaluate the sensitivity of global CCN to uncertainties associated with various nucleation parameterizations.

4. Summary and discussion

Simple empirical nucleation parameterizations, which were derived from laboratory or field measurements under limited conditions and do not consider any temperature dependence of nucleation rates, have been widely used in global aerosol modeling and aerosol indirect radiative forcing studies. Based on the classical nucleation theory, temperature should be one of key

parameters controlling nucleation rates, unless nucleation is barrierless. A recent study indicates (Yu et al., 2015) that the empirical parameterization of H_2SO_4-Organics nucleation of Riccobono et al. (2014) significantly over-predicts NPF and particle number concentrations in North America in summer. The lack of temperature dependence in the parameterization has been suggested as a likely reason for the observed over-prediction. In the present study, H_2SO_4-Organics clustering thermodynamics from quantum-chemical studies has been employed to develop a scheme for incorporating the temperature dependence into H_2SO_4-Organics nucleation parameterization, which reduces global mean nucleation rate in the boundary layer in a summer month is by a factor of ~ 8 and improves the agreement of predicted particle number concentrations over North America with observations. With temperature-dependent H_2SO_4-Organics nucleation parameterization, the summer month CCN concentrations in the lower troposphere in the northern hemisphere are about 10-30% lower. In view of the potential effects of changes in CCN concentrations on precipitation (second indirect impact) and cloud cover, it is important to reduce uncertainties in NPF calculation in regional and global climate models.

The study highlights the importance of including the temperature dependence of nucleation rates in global modeling of NPF and aerosol indirect radiative forcing. In a recent study, Dunne et al. (2016) also showed a substantial impact of the temperature dependence on the contribution of organic nucleation to overall nucleation. The temperature dependence factor derived under this study can be applied to study the temperature effect on organics-mediated nucleation in the global atmosphere and improve the agreement of simulated particle number concentrations with observations. Although it may subject to uncertainties due to the possible difference between the molecules involved in the nucleation and the proxy molecule, temperature dependent $J_{Nucl\text{-}OrgT}$, likely more realistic than $J_{Nucl\text{-}Org}$, in which the temperature dependence is neglected. Further

laboratory measurements and theoretical studies are needed to better understand the effect of temperature on organics-mediated nucleation in the atmosphere.

Acknowledgments. This study was supported by NASA under grant NNX13AK20G and the National Science Foundation (NSF) under grant 1550816. We would like to acknowledge high-performance computing support from Yellowstone (ark:/85065/d7wd3xhc) provided by NCAR's Computational and Information Systems Laboratory, sponsored by the NSF. The GEOS-Chem model is managed by the Atmospheric Chemistry Modeling Group at Harvard University with support from NASA's Atmospheric Chemistry Modeling and Analysis Program.

References

Bey, I., Jacob, D. J. Yantosca, R. M. , Logan, J. A. Field, B. Fiore, A. M. Li, Q., Liu, H., Mickley, L. J., and Schultz, M.: Global modeling of tropospheric chemistry with assimilated meteorology: Model description and evaluation, Journal of Geophysical Research, 106, 23,073–23,096, 2001.

DePalma, J. W., J. Wang, A. S. Wexler, and M.V Johnston, Growth of ammonium bisulfate clusters by adsorption of oxygenated organic molecules, The Journal of Physical Chemistry A, 119 (45), 11191–11198, DOI: 10.1021/acs.jpca.5b07744, 2015.

Dune et al., Global atmospheric particle formation from CERN CLOUD measurements, Science, 354, 6316, DOI:10.1126/science.aaf2649, 2016.

Elm, J., M. Bilde, and K. V. Mikkelsen: Assessment of binding energies of atmospherically relevant clusters. Physical Chemistry Chemical Physics 15.39, 16442-16445., 2013.

306 Elm, J., T. Kurten,´M. Bilde and K.V. Mikkelsen: Molecular interaction of pinic acid with
307 sulfuric acid: Exploring the thermodynamic landscape of cluster growth, The Journal of
308 Physical Chemistry A, 2014, 118, 7892−7900, 2014.
309 Frisch, M. J.; Trucks, G. W.; Schlegel, H. B.; Scuseria, G. E.; Robb, M. A.; Cheeseman, J. R.;
310 Scalmani, G.; Barone, V.; Mennucci, B.; et al.: Gaussian 09, Gaussian, Inc., Wallingford CT,
311 2009.
312 Herb, J., Y. Xu, F. Yu, and A. B. Nadykto, Large hydrogen-bonded pre-nucleation (HSO_4^-)
313 $(H_2SO_4)_m(H_2O)_k$ and $(HSO_4)(NH_3)(H_2SO_4)_m(H_2O)_k$ Clusters in the Earth's Atmosphere, The
314 Journal of Physical Chemistry A, *117* (1), 133–152, 2013.
315 IPCC, Climate Change 2013: The Physical Scientific Basis, edited by T. F. Stocker, D. Qin, et al.,
316 Cambridge Univ. Press, New York, USA, 2013.
317 Kazil, J., Stier, P., Zhang, K., Quaas, J., Kinne, S., O'Donnell, D., Rast, S., Esch, M., Ferrachat,
318 S., Lohmann, U., and Feichter, J.: Aerosol nucleation and its role for clouds and Earth's
319 radiative forcing in the aerosol-climate model ECHAM5-HAM, Atmospheric Chemistry and
320 Physics, 10, 10733-10752, doi:10.5194/acp-10-10733-2010, 2010.
321 Kuang, C., McMurry, P. H., McCormick, A. V., and Eisele, F. L.: Dependence of nucleation
322 rates on sulfuric acid vapor concentration in diverse atmospheric locations, J. Geophys. Res.,
323 113, D10209, doi:10.1029/2007JD009253, 2008.
324 Lupascu, A., Easter, R., Zaveri, R., Shrivastava, M., Pekour, M., Tomlinson, J., Yang, Q., Matsui,
325 H., Hodzic, A., Zhang, Q., and Fast, J. D.: Modeling particle nucleation and growth over
326 northern California during the 2010 CARES campaign, Atmos. Chem. Phys., 15, 12283-
327 12313, doi:10.5194/acp-15-12283-2015, 2015.

328 Metzger, A., Verheggen, B., Dommen, J., Duplissy, J., Prevot, A.S., Weingartner, E., Riipinen, I.,
329 Kulmala, M., Spracklen, D.V., Carslaw, K.S. and Baltensperger, U.: Evidence for the role of
330 organics in aerosol particle formation under atmospheric conditions, Proceedings of the
331 National Academy of Sciences, 107(15), pp.6646-6651, 2010.
332 Nadykto, A. B., J. Herb, F.Yu, and Y. Xu: Enhancement in the production of nucleating clusters
333 due to dimethylamine and large uncertainties in the thermochemistry of amine-enhanced
334 nucleation, Chemical Physics Letters, 609, 42-49, 2015.
335 Pierce, J.R., and Adams, P.J.: Uncertainty in global CCN concentrations from uncertain aerosol
336 nucleation and primary emission rates, Atmospheric Chemistry and Physics, 9, 1339-1356,
337 2009.
338 Pillai, P., Khlystov, A., Walker, J. and Aneja, V. Observation and analysis of particle nucleation
339 at a forest site in southeastern US. Atmosphere. 4(2):72-93, 2013.
340 Riccobono, FSchoberberger, S., Scott, C.E., Dommen, J., Ortega, I.K., Rondo, L., Almeida, J.,
341 Amorim, A., Bianchi, F., Breitenlechner, M., David, A., Downard, A., Dunne, E.M.,
342 Duplissy, J., Ehrhardt, S., Flagan, R.C., Franchin, A., Hansel, A., Juuninen, H., Kajos, M.,
343 Keskinen, H., Kupc, A., Kürten, A., Kvashin, A.N., Laaksonen, A., Lehtipalo, K.,
344 Makkmutov, V., Mathot, S., Nieminen, T., Onnela, A., Petäjä, T.,Praplan, A.P., Santos, F.D.,
345 Schallhart, S., Seinfeld, J.H., Sipilä, M., Spracklen, D.V., Stozhkov, Y., Stratmann, F., Tomé,
346 A., Tsagkogeorgas, G., Vaattlovaara, P., Viisanen, Y., Vrtala, A., Wagner, P.E., Weingartner,
347 E., Wex, H., Wimmer, D., Carslaw, K.S., Curtius, J., Donahue, N.M., Kirkby, J., Kulmala, M.
348 Worsnop, D.R., and Baltensperger, U.: Oxidation products of biogenic emissions contribute
349 to nucleation of atmospheric particles, Science, 344, 717, 2014.

Riipinen, I., S.-L. Sihto, M. Kulmala, F. Arnold, M. Dal Maso, W. Birmili, K. Saarnio, K. Teinilä, V.-M. Kerminen, A. Laaksonen, and K. E. J. Lehtinen: Connections between atmospheric sulphuric acid and new particle formation during QUEST III–IV campaigns in Heidelberg and Hyytiälä, Atmos. Chem. Phys., 7, 1899-1914, 2007.

Scott, C. E., Rap, A., Spracklen, D. V., Forster, P. M., Carslaw, K. S., Mann, G. W., Pringle, K. J., Kivekäs, N., Kulmala, M., Lihavainen, H., and Tunved, P.: The direct and indirect radiative effects of biogenic secondary organic aerosol, Atmos. Chem. Phys., 14, 447-470, doi:10.5194/acp-14-447-2014, 2014.

Spracklen, D. V., Carslaw, K. S., Kulmala, M., Kerminen, V.-M.,Sihto, Riipinen, I., Merikanto, J., Mann, G.W., Chipperfield, M.P., Wiedensohler, A., Birmili, W., and Lihavainen, H.: Contribution of particle formation to global cloud condensation nuclei concentrations, Geophysical Research Letters, 35, L06808, doi:10.1029/2007GL033038, 2008.

Wang, M. and Penner, J. E.: Aerosol indirect forcing in a global model with particle nucleation, Atmospheric Chemistry and Physics, 9, 239–260, 2009.

Westervelt, D. M., Pierce, J. R., and Adams, P. J.: Analysis of feedbacks between nucleation rate, survival probability and cloud condensation nuclei formation, Atmos. Chem. Phys., 14, 5577-5597, doi:10.5194/acp-14-5577-2014, 2014.

Yu, F.: A secondary organic aerosol formation model considering successive oxidation aging and kinetic condensation of organic compounds: global scale implications, Atmospheric Chemistry and Physics, 11, 1083-1099, doi:10.5194/acp-11-1083-2011, 2011.

Yu, F., and G. Luo: Simulation of particle size distribution with a global aerosol model: contribution of nucleation to aerosol and CCN number concentrations. Atmospheric Chemistry and Physics, 9, 7691-7710, 2009.

373 Yu, F., G. Luo , T. Bates , B. Anderson , A. Clarke , V. Kapustin , R. Yantosca , Y. Wang , S.
374 Wu: Spatial distributions of particle number concentrations in the global troposphere:
375 Simulations, observations, and implications for nucleation mechanisms, J. Geophys. Res.,
376 115, D17205, doi:10.1029/2009JD013473, 2010.
377 Yu, F., Luo, G., Liu, X., Easter, R. C., Ma, X., and Ghan, S. J.: Indirect radiative forcing by ion-
378 mediated nucleation of aerosol, Atmospheric Chemistry and Physics, 12, 11451-11463, 2012.
379 Yu, F., X. Ma, and G. Luo: Anthropogenic contribution to cloud condensation nuclei and the
380 first aerosol indirect climate effect, Environmental Research Letters 8 024029
381 doi:10.1088/1748-9326/8/2/024029, 2013.
382 Yu, F., Luo, G., Pryor, S. C., Pillai, P. R., Lee, S. H., Ortega, J., Schwab, J. J., Hallar, A. G.,
383 Leaitch, W. R., Aneja, V. P., Smith, J. N., Walker, J. T., Hogrefe, O., and Demerjian, K. L.:
384 Spring and summer contrast in new particle formation over nine forest areas in North
385 America, Atmos. Chem. Phys., 15, 13993-14003, doi:10.5194/acp-15-13993-2015, 2015.
386 Zhang, R., I. Suh, J. Zhao, D. Zhang, E.C. Fortner, X. Tie, L.T. Molina, and M.J. Molina:
387 Atmospheric new particle formation enhanced by organic acids**,** Science, 304, 1487-1490,
388 2004.
389
390
391

392 Table 1. Changes of enthalpy (ΔH), entropy (ΔS), and Gibbs free energy (ΔG) for the formation

393 of $(C_{10}H_{14}O_7)$ $(H_2SO_4)_2$ cluster under the standard condition (P= 1 atm, T=298 K).

	ΔH (kcal mol^{-1})	ΔS (cal $mol^{-1}K^{-1}$)	ΔG (kcal mol^{-1})
$C_{10}H_{14}O_7 + H_2SO_4 + H_2SO_4 \leftrightarrows (C_{10}H_{14}O_7)(H_2SO_4)_2$	-38.30	-75.45	-15.81

394

Figure Captions

Figure 1. Equilibrium geometry of the most stable isomers of heteromolecular trimer composed of $(C_{10}H_{14}O_7)$ $(H_2SO_4)_2$ obtained at PW91PW91/6-311++G(3df,3pd) level of theory. Bonding lengths are in angstroms.

Figure 2. Calculated temperature dependence correction factor for Nucl-Org parameterization (f_T) as a function of T.

Figure 3. Horizontal distributions of monthly mean nucleation rates (J) (a, b), concentrations of condensation nuclei larger than 10 nm (CN10) (c, d), and concentrations of cloud condensation nuclei at water supsaturation ratio of 0.4% (CCN0.4) (e, f) in the boundary layer (0-1 km above the surface) in July of 2006 based on two organics-mediated nucleation schemes: $J_{Nucl\text{-}Org}$ (left panels) and $J_{Nucl\text{-}OrgT}$ (right panels).

Figure 4. Dependence of organics-mediated nucleation rates (left axis), CN10 and CCN0.4 (right-axis) averaged in the boundary layer (0-1 km) over the whole globe for July 2006 on ΔH values assumed in calculating temperature dependence correction factor for Nucl-Org parameterization (f_T).

Figure 5. Horizontal distributions of monthly mean CN10 in the boundary layer (0-1 km above surface) in July of 2006 based on two organics-mediated nucleation schemes: (a) $J_{Nucl\text{-}Org}$ and (b) $J_{Nucl\text{-}OrgT}$. The locations of 9 forest sites where observed particle size distributions measurements have been used for comparisons in Yu et al. (2015) are marked.

Figure 6. Effect of ΔH values on simulated number concentrations of condensation nuclei in the size range of 10 and 100 nm ($CN_{10\text{-}100}$) in the boundary layer (0-1 km) for July 2006 averaged over nine forest sites in North America (NA) (locations marked on Fig. 5). The horizontal dashed line shows the average of $CN_{10\text{-}100}$ observed in a summer month at the 9 sites.

418 **Figure 7.** Particle size distributions (PSDs) observed (a, b) and simulated based on Nucl-Org (c,
419 d) and Nucl-OrgT (e, f) schemes during two ten-day periods in March (a, c, e) and July (b, d, f)
420 of 2006 in Duke Forest (DUK), along with time series of the concentration of condensation
421 nuclei between 10 and 100 nm ($CN_{10\text{-}100}$) (g, h).
422 **Figure 8.** Ratios of the concentration of CCN (at water supersaturation ratio of 0.2%) in the
423 lower troposphere (0-3 km) based on Nucl-Org scheme to those based on Nucl-OrgT scheme.
424

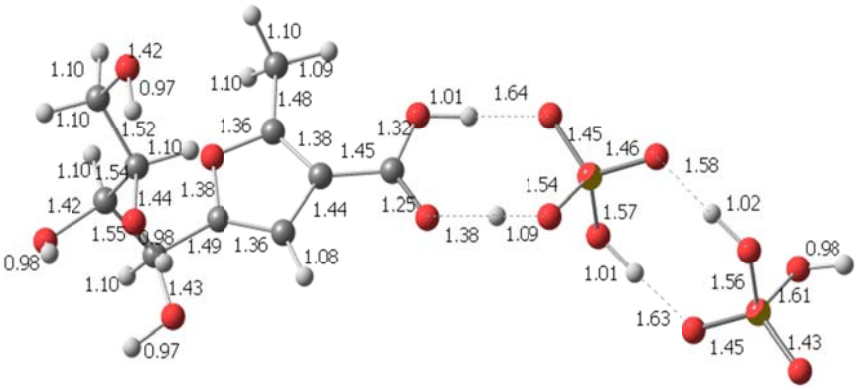

Figure 1.

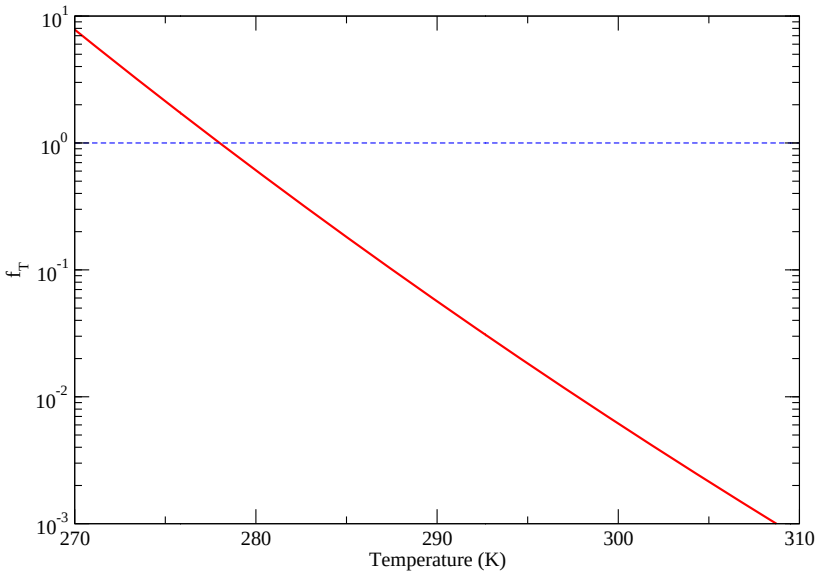

Figure 2.

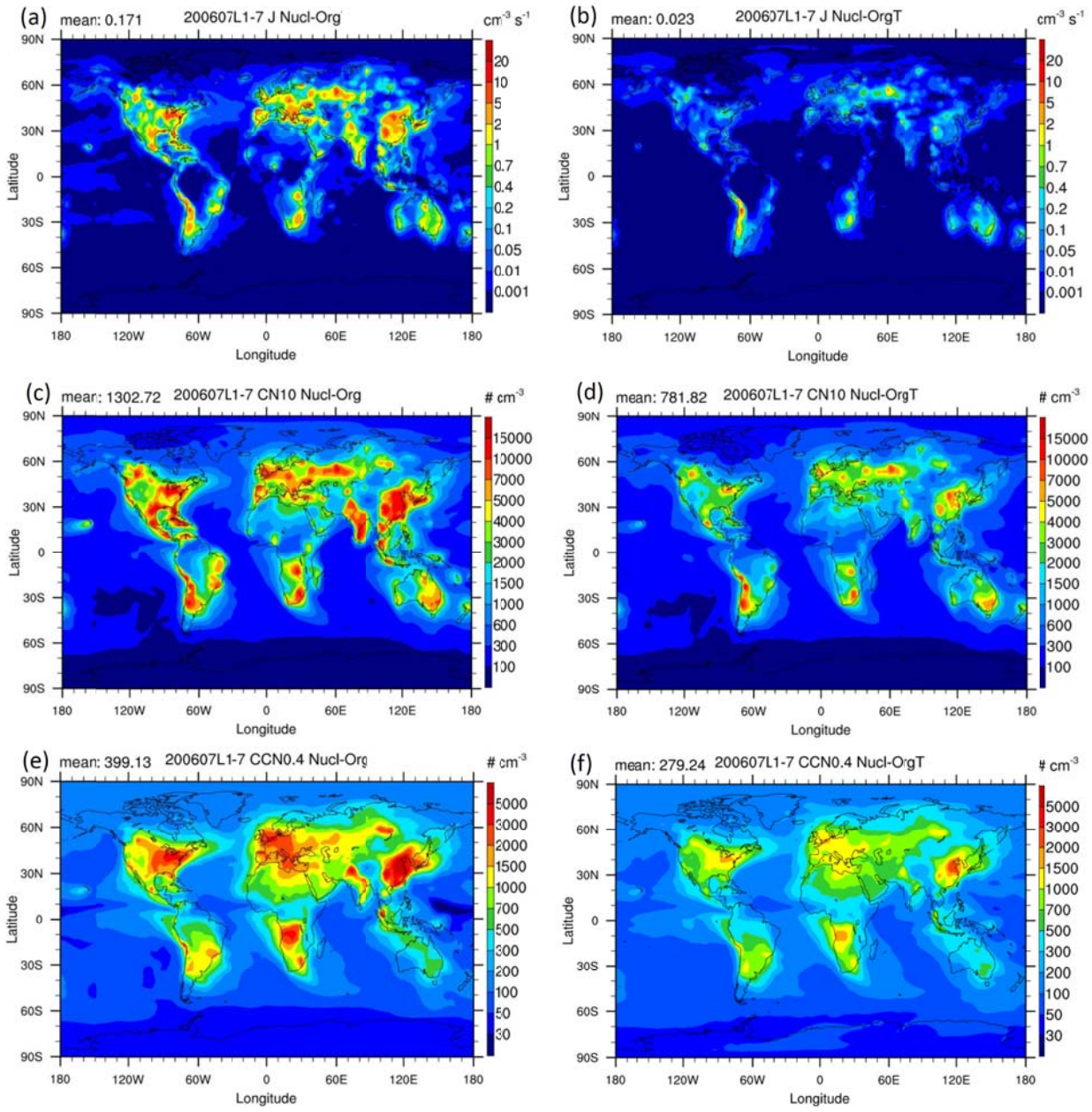
(a) mean: 0.171 200607L1-7 J Nucl-Org
(b) mean: 0.023 200607L1-7 J Nucl-OrgT
(c) mean: 1302.72 200607L1-7 CN10 Nucl-Org
(d) mean: 781.82 200607L1-7 CN10 Nucl-OrgT
(e) mean: 399.13 200607L1-7 CCN0.4 Nucl-Org
(f) mean: 279.24 200607L1-7 CCN0.4 Nucl-OrgT
Latitude
Longitude
90N
60N
30N
0
30S
60S
90S
180
120W
60W
0
60E
120E
180
cm-3 s-1
cm-3

Figure 3.

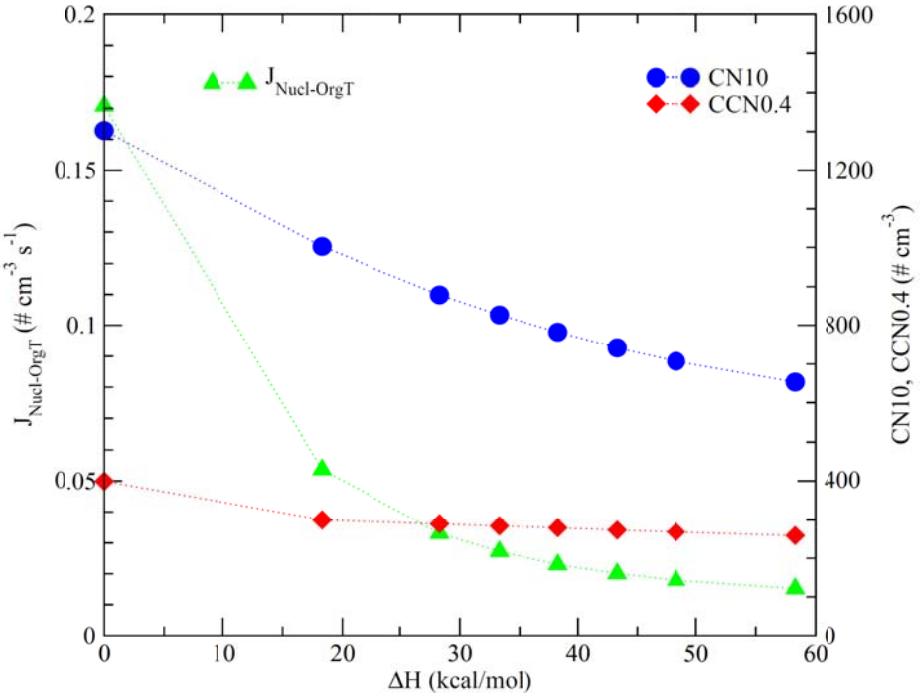

Figure 4.

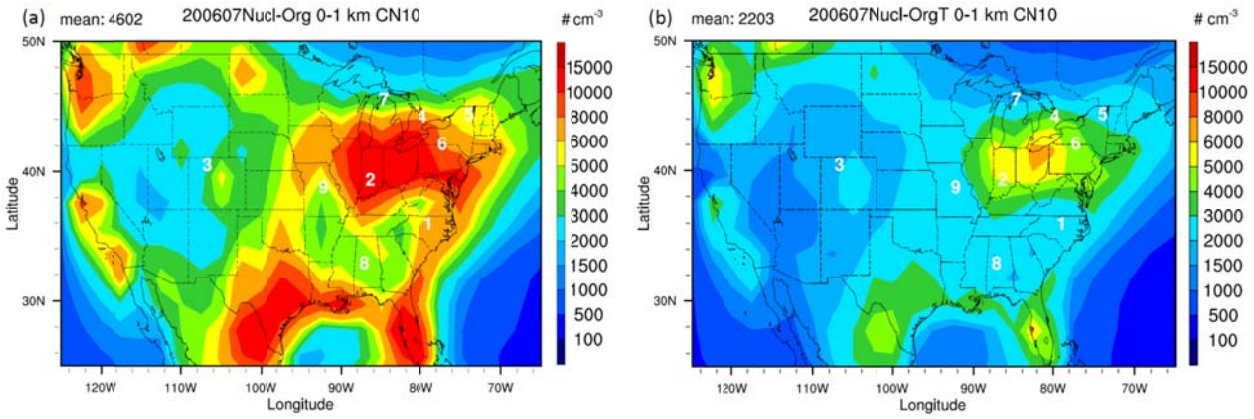

Figure 5.

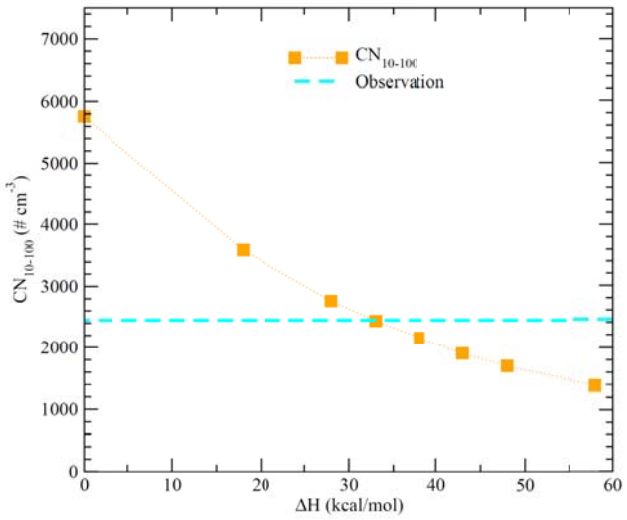

455

456 Figure 6.

457

458

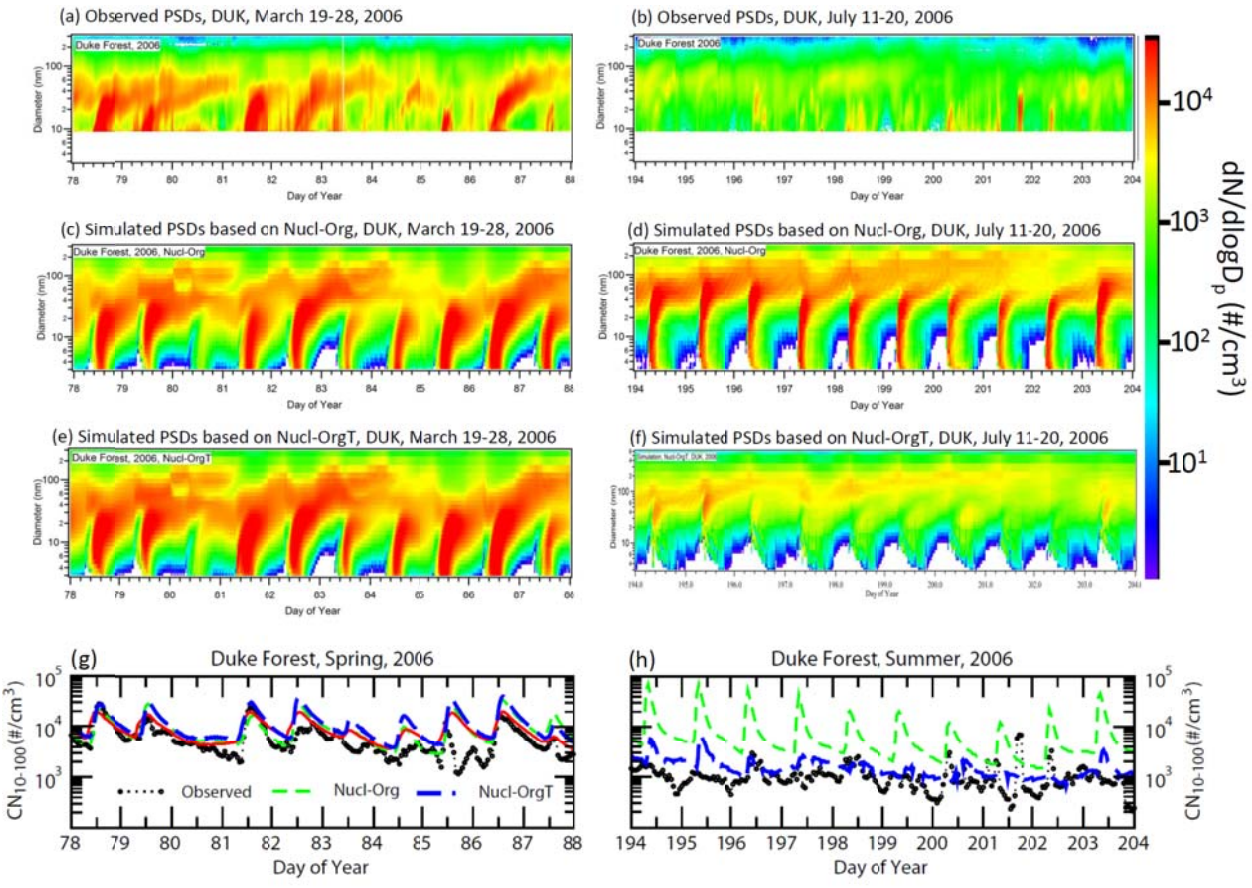

459

460 Figure 7.

461

462

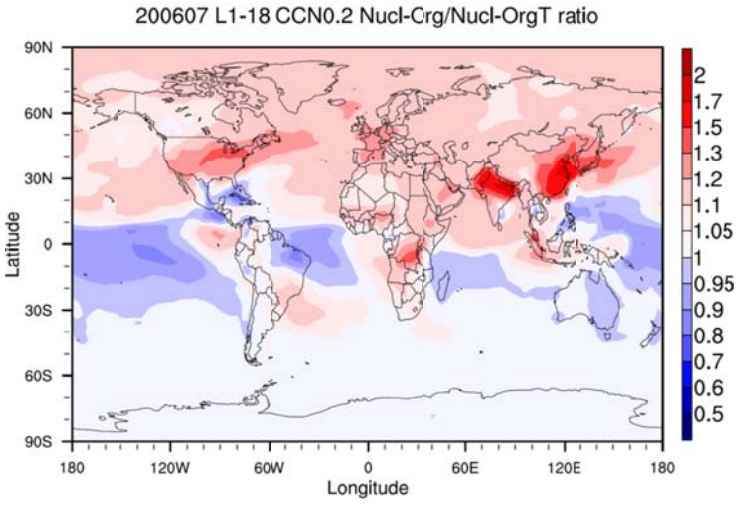

463

464 Figure 8.

465